PSYCHOPHYSIOLOGY

Psychophysiology, 00 (2016), 00–00. Wiley Periodicals, Inc. Printed in the USA.

DOI: 10.1111/psyp.12814

An information theory account of late frontoparietal ERP positivities in cognitive control

AQ1 FRANCISCO BARCELÓ[a] AND PATRICK S. COOPER[b,c]

[a]Laboratory of Neuropsychology, University of the Balearic Islands, Mallorca, Spain
[b]Functional Neuroimaging Laboratory, School of Psychology, University of Newcastle, Callaghan, Australia
[c]Priority Research Centre for Brain and Mental Health, University of Newcastle, Callaghan, Australia

Abstract

ERP research on task switching has revealed distinct transient and sustained positive waveforms (latency circa 300–900 ms) while shifting task rules or stimulus-response (S-R) mappings. However, it remains unclear whether such switch-related positivities show similar scalp topography and index context-updating mechanisms akin to those posed for domain-general (i.e., classic P300) positivities in many task domains. To examine this question, ERPs were recorded from 31 young adults (18–30 years) while they were intermittently cued to switch or repeat their perceptual categorization of Gabor gratings varying in color and thickness (switch task), or else they performed two visually identical control tasks (go/no-go and oddball). Our task cueing paradigm examined two temporarily distinct stages of proactive rule updating and reactive rule execution. A simple information theory model helped us gauge cognitive demands under distinct temporal and task contexts in terms of low-level S-R pathways and higher-order rule updating operations. Task demands modulated domain-general (indexed by classic oddball P3) and switch positivities—indexed by both a cue-locked late positive complex and a sustained positivity ensuing task transitions. Topographic scalp analyses confirmed subtle yet significant split-second changes in the configuration of neural sources for both domain-general P3s and switch positivities as a function of both the temporal and task context. These findings partly meet predictions from information estimates, and are compatible with a family of P3-like potentials indexing functionally distinct neural operations within a common frontoparietal "multiple demand" system during the preparation and execution of simple task rules.

Descriptors: Context updating, Executive function, Information theory, P300, Task-set inertia, Task-set reconfiguration

ERPs measured during task switching have consistently shown several distinct positive waveforms present when shifting task rules/stimulus-response (S-R) mappings (e.g., Karayanidis, Coltheart, Michie, & Murphy, 2003; Karayanidis et al., 2009; Karayanidis, Provost, Brown, Paton, & Heathcote, 2011; Rushworth, Passingham, & Nobre, 2002). These ERP positivities, which typically occur 300–900 ms postswitch stimulus, are often interpreted as reflecting switch-specific control processes (Kopp & Lange, 2013; Lavric, Mizon, & Monsell, 2008; Nicholson et al., 2011). However, some authors have suggested switch positivities may actually have a functional relationship with the ubiquitous P300 component observed across many task domains (hereafter, the *domain-general* P3), probably reflecting higher-order context-updating mechanisms akin to those hypothesized for P3 potentials in simpler target detection tasks (Barceló, Escera, Corral, & Periáñez, 2006; Barceló, Periáñez, & Knight, 2002; Barceló, Periáñez, & Nyhus, 2008; Kieffaber & Hetrick, 2005; cf. Donchin, 1981).

Switch-related and P300 positivities appear to have similar scalp topographies, suggesting they both recruit activity from a common cluster of frontoparietal regions (Bledowski et al., 2004). Given that frontoparietal networks are readily associated with cognitive control across many task domains (Cole et al., 2013; Petersen & Posner, 2012), the notion of such a "multiple demand" system (Duncan, 2013) may underpin the link between P3 and switch potentials. While many authors have interpreted the similar scalp topographies between the canonical P300 and switch positivities as reflecting context-updating mechanisms akin to those posited for P300 elicitation (Barceló et al., 2008; Kieffaber & Hetrick, 2005), to date this link remains unconfirmed. Few ERP studies have directly examined whether switch positivities are comparable to the canonical P300 both in their scalp topographies and in their purported context-updating function across task domains (cf. Holig & Berti, 2010; Lavric et al., 2008).

This study was supported by grants from Fundació La Marató de TV3 (112710) and Spanish Ministry of Economy and Competitiveness (MINECO PSI2013-44760-R) (FB). We thank Javier Villacampa, Rosa Martorell, Marcelina Chamielec, and Álvaro Darriba for their contribution to task programming, recruitment, data collection, and EEG signal preprocessing.

Address correspondence to: Francisco Barceló, PhD., Laboratory of Neuropsychology, University of the Balearic Islands, 07122 Palma de Mallorca, Balearic Islands, Spain. E-mail: f.barcelo@uib.es

Many practical difficulties hinder progress toward a theoretical integration of domain-general P3 and switch positivities. First, one prominent issue is the temporal contingencies among task stimuli and responses (i.e., the "temporal context" of goal-directed actions; Fuster, 2001). For example, in oddball paradigms, it is widely accepted that P300 potentials can be elicited by both the targets of goal-directed behavior and by infrequent oddball distracters that are not to be responded to (Polich, 2007; Squires, Squires, & Hillyard, 1975). These targets and rare distracters elicit two functionally distinct P300 potentials whose scalp topographies differ along a frontoparietal axis, with a more centroparietal scalp distribution for the former and a more frontal distribution for the latter (Polich & Comerchero, 2003; Spencer, Dien, & Donchin, 1999). However, many P300 studies use oddball targets and thus confound the "oddballness" and "targetness" aspects of cognitive control, akin to the stages of proactive strategic preparation and reactive execution of simple sensorimotor rules, as defined in task-cueing paradigms (Braver, 2012). That is, when an oddball target occurs within a sequence of repetitive standard distracters, one has to process its oddballness first, and then process its target or distracter features in order to select the appropriate motor response, and these two processes overlap in the summated ERP waveforms. Therefore, to clarify whether the frontal and parietal aspects of P300 index strategic resolution of contextual uncertainty (oddballness), as distinct from reactive execution of simple sensorimotor rules (targetness), targets need to be presented at predictable intervals within the trial run. Task-cueing procedures have revealed distinct frontoparietal switch positivities for these two distinct processing stages, with parietal maxima to temporally predictable targets during rule execution, and more anterior maxima to infrequent unpredictable task cues that anticipate a switch in rules (Barceló et al., 2002; Kieffaber & Hetrick, 2005). This evidence highlights the temporal dynamics of two distinct modes for the control of task switching, with proactive rule updating and reactive rule execution stages differentially engaging the frontoparietal control network (Braver, 2012). Presumably, these same temporal dynamics also apply in simpler task domains. For instance, proactive interference in first target trials following an unexpected interruption has been proposed as a prime determinant of residual (restart) costs under single task conditions (Allport, Styles, & Hsieh, 1994; Barceló et al., 2008).

A second key limitation toward an integrative view of the P300 and switch positivities is the strict dichotomy between the two subcomponents of the P300, with the frontal P3a linked to rare, novel, and ignored stimuli, and the centroparietal P3b linked to attended, relevant, and consciously processed stimuli (for a review, see Polich, 2007). Such a sharp and dichotomous taxonomy impedes a theoretical integration of P3a/P3b subcomponents with modern views about a graded contribution from both frontal and temporoparietal nodes of frontoparietal cortical networks, while dealing with a continuum of gradually increasing cognitive demands (Bledowsky et al., 2004; Cole et al., 2013). For example, Barceló et al. (2006) used principal component analysis (PCA) to demonstrate that P3-like potentials to irrelevant novel sounds and relevant tones that signaled an upcoming task switch both showed similar peak latencies and scalp topographies, with more frontal or parietal maxima depending on their task context (for P3a potentials with parietal maxima, see Kopp & Lange, 2013; Polich, 2007). This finding suggests that both irrelevant novel stimuli and familiar task cues may evoke a gradient of activity across frontal and parietal regions depending on their task context. Here, we assume a common frontoparietal network for dealing with a whole gamut of cognitive demands beyond the traditional extreme "ignore" versus "attend" dichotomy (Barceló & Knight, 2007).

A third limitation is the use of notional rather than formal definitions of context, which hinders examination of the prevailing "context-updating" hypothesis of P300 (Donchin, 1981) across different task contexts, and impedes a direct comparison with switch positivities. Traditional views consider the stimulus context (i.e., mean stimulus probability) to be a major determinant of P300 amplitudes (Polich, 2007). However, the above examples highlight the influence of both temporal and task contexts on frontoparietal P300 dynamics, as a function of the cognitive demands associated with similar stimuli delivered under different task contexts. This highlights the importance of S-R links and sensorimotor information transmission—over and above stimulus properties alone—to completely explore the link between P3 and switch positivities (Verleger, Baur, Metzner, & Smigasiewicz, 2014; Verleger, Jaskowoski, & Wäscher, 2005). To this end, here we adopted a simple model of cognitive control based on information theory to compare cognitive demands associated with equally infrequent gray Gabor gratings, which set the temporal context for implementing the same visuomotor rule upon ensuing colored Gabor gratings delivered under three different task contexts (switch, go/no-go, and oddball tasks). This approach helped us to mathematically operationalize the construct of context updating (Donchin, 1981) and to control for the confound between oddballness and targetness by factoring out the influence of the temporal context on neural activity and behavior. In doing so, we estimated the sensorimotor information transmitted between contextually related task stimuli and their associated motor responses (or "input-output correlations"; Miller, 1956) at both lower- and higher-order levels in a putative hierarchy of sensorimotor control (cf. Barceló & Knight, 2007, 2008).

Information theory allows us to assign task properties binary digit values or bits (Attneave, 1959; Cooper, Garrett, Rennie, & Karayanidis, 2015). In this way, S-R contingencies can be ascribed an information value, permitting simple contrasts between tasks. Information theory allows us to gauge cognitive demands associated with dissimilar stimulus and response sets, and distinct S-R mappings in order to predict the intensity and scalp topography of ERP positivities across different task domains. For instance, Barceló et al. (2008) relied on information theory estimates to demonstrate the distinct functional roles of cue-locked (i.e., context) P3 and target P3 potentials elicited by the same sequence of red and blue shapes interspersed with infrequent black symbols administered under oddball, go/no-go, and task-cueing instructions. These authors found similar frontocentral scalp topographies—albeit with different magnitudes—for context-related P3s and switch positivities to the infrequent black symbols, consistent with their information estimates. In sharp contrast, target P3 amplitudes were not modulated by task demands, and showed similar midparietal amplitudes and topographies across all task contexts. Thus, hereafter we will adopt the term *context P3* to describe positivities elicited by infrequent gray Gabor gratings that are predicted to index context-updating operations proactively, in anticipation of target onset, and regardless of the task context. Conversely, we will adopt the term *target P3* to describe ERP positivities elicited by temporally predictable colored gratings thought to recruit mostly reactive target detection, without the temporal unpredictability of oddball targets. Finally, we circumvent limitations of an earlier study (Barceló et al., 2008) by using a within-subject task design, larger sample sizes, and surface Laplacian values to minimize volume conduction of scalp potentials.

In sum, this study aimed to examine the similarities and differences in the intensities and scalp distribution of domain-general P3 (300–400 ms) and switch-related (300–900 ms)[1] ERP positivities, while participants were intermittently cued to switch or repeat their categorization of Gabor gratings varying in color and thickness (switch task). Two perceptually identical tasks served as controls with varying cognitive and response demands (go/no-go and oddball). Following the discussion above, we addressed one important question: Are switch positivities topographically similar and functionally compatible with a context-updating mechanism akin to that proposed for the canonical P3 component recorded in simpler oddball and go/no-go tasks? This question was addressed by testing two specific hypotheses: (1) If the temporal context of goal directed actions (i.e., proactive strategic preparation vs. reactive execution of a simple visuomotor rule) modulates the frontoparietal scalp distribution of late P3-like positivities, then more frontal positivities will be elicited during proactive preparation (e.g., higher-order rule updating) than during lower-order sensorimotor control of reactive rule execution at target onset (Barceló et al., 2008; Braver, 2012). (2) If the parametric increase in cognitive demands posed by three different task contexts (oddball, go/no-go, switch) modulates the frontoparietal distribution and magnitude of late P3-like positivities, then gradually more frontal positivities will be elicited with gradually higher cognitive demands, in line with predictions from an information theory model of cognitive control (Koechlin & Summerfield, 2007). These two predictions relied on the hypothetical contribution from a common frontoparietal multiple demand system (Duncan, 2013) to both domain-general P3 and switch P3-like positivities. To test these two hypotheses, we recorded P3 potentials to oddball and go/no-go Gabor gratings and compared their scalp distributions with switch P3-like potentials to identical stimuli delivered under switch task conditions. To favor integration with the extant literature, we analyzed mean amplitudes and surface Laplacian values from four midline regions (frontopolar, frontal, central, and parietal), under the assumption that distinct scalp topographies and functional dissociations to experimental factors characterize distinct ERP components (Kappenman & Luck, 2012). For simplicity, we modeled sensorimotor information transmission only at two levels in the putative hierarchy of cognitive control, namely, low-level sensorimotor control (i.e., changes in single S-R pathways) and higher-order episodic control of task rule retrieval and updating (Dayan, 2007; see online supporting information).

Method

Participants

Thirty-one participants (25 female, $M_{\text{age}} = 21.8$ years ± 2.7 *SD*) took part in the current study and received course credit for their collaboration. All were graduate or postgraduate students at the University of the Balearic Islands with normal or corrected-to-normal vision and reported no history of neurological or psychiatric disorders. Informed consent was obtained from all participants, and experimental procedures and behavioral testing was performed in accordance with the Declaration of Helsinki and the approval of the Ethics committee of the university.

Stimulus Materials and Procedures

Participants sat in a sound-attenuated and dimly lit room at a viewing distance of 150 cm from a 27-inch video LCD monitor (800×600 at 75 Hz). Stimuli were displayed against a gray background (2.85 cd/m^2) at a visual angle of 6.5° to the left or right of a central fixation cross with $0.5^\circ \times 0.5^\circ$ of visual angle.[2] A central fixation cross remained continuously present throughout each experimental run. Stimuli consisted of four equally probable ($p = 0.21$), colored Gabor gratings with horizontally oriented gratings (either red or blue, 4 or 10 cpd [circles per degree], 25% contrast, 1° visual angle, 3.5 cd/m^2), and two infrequent ($p = .08$) gray Gabor gratings (oriented either vertically or horizontally, 2 cpd, 25% contrast, 1° visual angle, 3.5 cd/m^2). Participants responded via a handheld response pad with their left or right index finger.

The experimental procedures have been described elsewhere (Cooper, Darriba, Karayanidis, & Barceló, 2016), and consisted of three different tasks: switch, go/no-go, and oddball, yoked for stimuli and trial sequences but involving different response and cognitive demands each (Figure 1). A test sequence included 976 trials of colored and gray Gabor gratings that was semirandomly generated offline, with the constraint that consecutive gray Gabor gratings were separated by four to eight colored gratings. This trial sequence was divided into eight blocks to allow for short, self-paced breaks approximately every 5 min. Each trial consisted of a Gabor grating presented for 100 ms in the left or the right visual hemifield. On designated target trials, participants had to respond within a maximum of 1,200 ms after stimulus onset. Instructions emphasized both response speed and accuracy. All error trials (i.e., incorrect, late responses, and false alarms) were followed by visual feedback, and the following trial was delayed by 500 ms to help subjects keep on task. Hence, stimulus onset asynchrony was either 1,900 or 2,400 ms on correct and error trials, respectively. The present ERP analyses were based on correct trials only. The stimulus display and behavioral response recording were implemented using Presentation software (Neurobehavioral Systems Inc., Albany, CA).

Each participant was presented with a unique, pseudorandomly generated test sequence that was repeated three times under different task instructions for the oddball, go/no-go, and switch tasks. Tasks were administered in counterbalanced order to control for inadvertent order effects. Thus, the three tasks involved an identical stimulus context but different cognitive and response demands (Figure 1).

The switch task (Figure 1A) was a variant of the intermittent-instruction paradigm (Monsell, 2003; Rushworth et al., 2002). The gray Gabor stimuli were cues, indicating whether to switch or repeat the task. The colored Gabor stimuli were targets and required a left- or right-hand response based on either the color (blue or red grating) or the grating's spatial frequency (thick or thin grating). Hence, the orientation of the gray grating (cue) instructed participants whether to switch or repeat the task they completed on the previous trial run. Gray grating orientations and instructions

---

[1] As clarified in Method, the distinction between domain-general and switch-related P3-like positivities relied on their sensitivity to experimental factors (i.e., switch vs. repeat trials) and on their distinct scalp topographies. However, given the large variability in the latency of P300 potentials with task complexity (Kutas, McCarthy, & Donchin, 1977), latency was not regarded as a criterion to differentiate ERP positivities (Kappenman & Luck, 2012), and switch positivities were sampled from a wider (300–900 ms) latency window, consistent with previous task-switching studies.

[2] A bilateral display was intended to assess hemispatial attention deficits in unilateral brain lesioned patients (cf. Barceló & Knight, 2007). A pilot study showed this bilateral display did not modulate late switch ERP positivities relative to a more conventional central display.

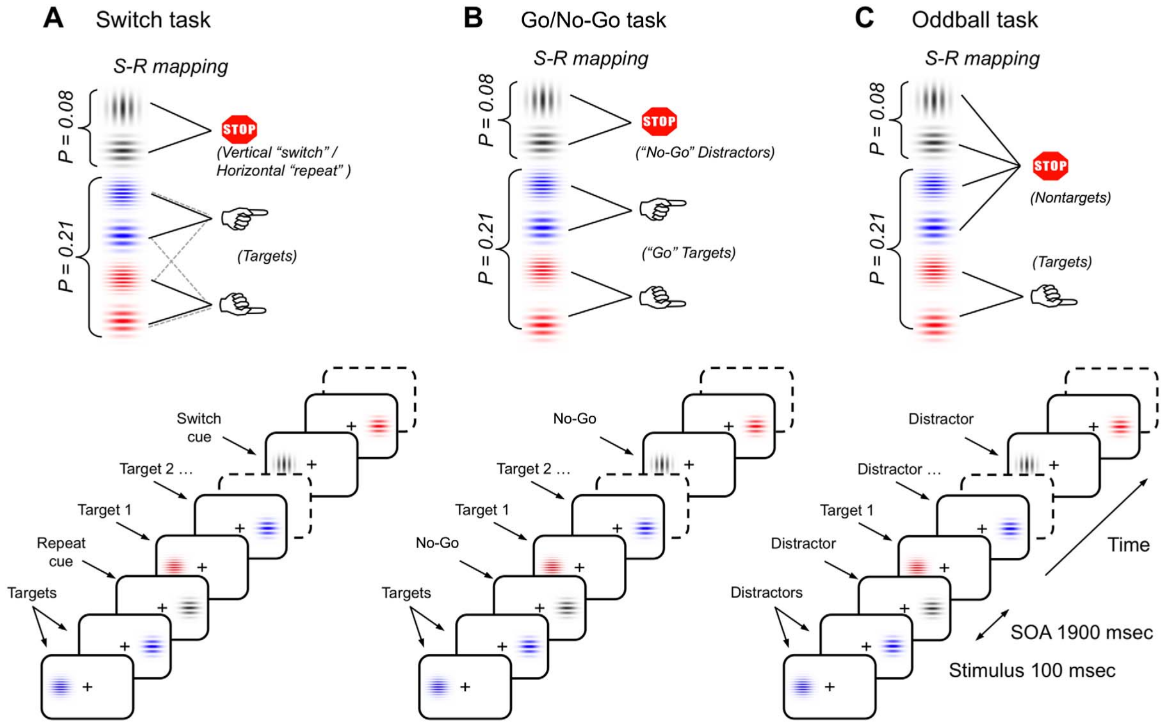

Figure 1. Task design, stimulus material, and S-R mappings. All three tasks consisted of the same sequence of frequent color gratings with semirandomly interspersed infrequent gray gratings. A: In the switch task, vertical and horizontal gray gratings instructed participants to switch and repeat the previous S-R mapping, respectively. B: The go/no-go task consisted of two-forced choice responses (Press button 1 for red gratings and button 2 for blue gratings). C: The oddball task involved one-forced choice responses (i.e., Press a button for all red gratings). Participants were explicitly instructed not to respond to the gray Gabor gratings. Hypothetical task-set information and S-R mappings for correct performance are also shown for each task. Cognitive demands were manipulated by (1) varying the amount of task-set information to be handled in working memory (oddball vs. go/no-go task), and (2) varying the type of contextual information conveyed by the gray gratings for anticipatory updating of active S-R mappings (go/no-go vs. switch task).

were counterbalanced between participants. A short training session was administered to ensure that participants reached a criterion of 80% correct responses and had understood task instructions.

The go/no-go task (Figure 1B) served as a control for the switch task. It involved an identical stimulus sequence and, again, participants responded only to the colored Gabors. However, importantly, here the gray Gabors had no predictive significance regarding the task to be performed, but set the temporal context for the next target onset. Rather they were defined as no-go stimuli, and participants were asked to withhold their response while implementing color classifications across the entire block of trials. In essence, this task is similar to a single-task block. In sum, the go/no-go task involved sorting Gabors by their color, an identical stimulus sequence and similar S-R mappings as the switching task.

The oddball task (Figure 1C) served as a control for both switch and go/no-go tasks, having an identical stimulus context but with different response demands. Specifically, a response was required only to red Gabor gratings, which were defined as oddball targets. All other stimuli did not require a motor response. This oddball task was inspired on regular novelty oddball tasks (Barceló & Knight, 2007), except that all targets, standard, and rare distracters included an additional irrelevant stimulus dimension (e.g., thickness of gratings).

Information Theory Estimations

We adopted an information theory approach to cognitive control as a formal tool to help us operationalize both temporal and task contexts in terms of low- and high-order sensorimotor (S-R) information transmission within a putative hierarchy of frontoparietal control processes (cf. Barceló & Knight, 2007; Cooper et al., 2016). These estimates allowed us to define the informational structure of our tasks in terms of not only mean stimulus probabilities, but also joint and conditional probabilities among stimuli, their associated motor responses, and any relevant cognitive operations involved (e.g., rule updating). Thus, the task context was modeled at two hierarchically distinct levels: (1) low-level sensorimotor control of single s-r pathways, and (2) higher-order episodic control of task rule updating (Dayan, 2007; Koechlin & Summerfield, 2007). The temporal context was separately modeled for infrequent gray Gabors and for the relatively more frequent colored Gabors. Thus, while infrequent gray Gabors were visually identical in all tasks, and appeared with identical probability, the type of information provided varied. Oddball gray Gabors transmitted the lowest sensorimotor information for response selection (as they did not anticipate target onset on the following trial) and no episodic information, given that the same task rule was used for all oddball targets and nontarget distractors. Alternatively, increased sensorimotor information was conveyed by no-go gray Gabors, as these stimuli were associated with less frequent no-go responses (r_0) compared to the oddball task, and they did anticipate target onset on the next trial. As with gray Gabors in the oddball task, no episodic information can be assumed for no-go gray Gabors given that the same task rule was consistently used across all trials. Finally, similar sensorimotor information was transmitted by all gray Gabors in the switch task, plus an additional amount of episodic

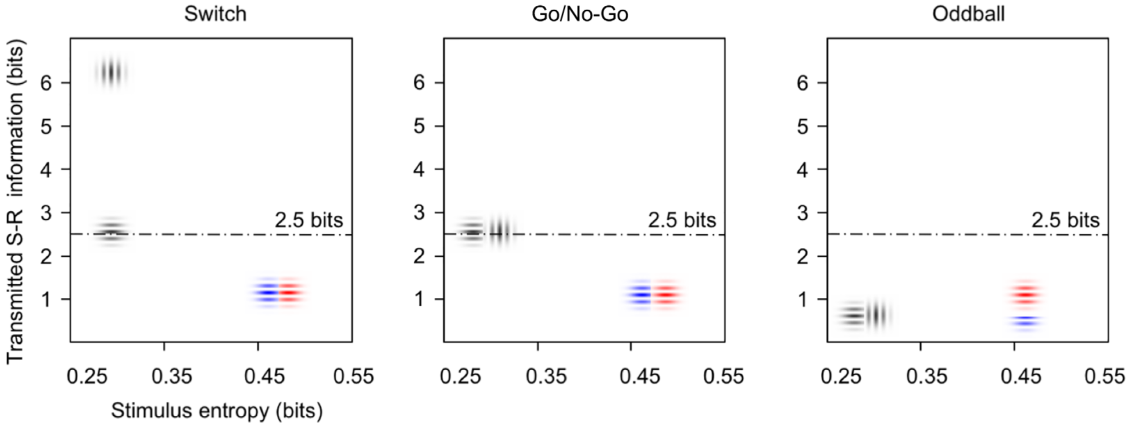

Figure 2. A priori estimations of transmitted information, $I(s_i, r_j)$, between stimuli and responses as a function of the sensory entropy, $H(s_i) = -p(s_i) \cdot \log_2 p(s_i)$, of gray and color gratings in the three tasks (or input-output correlations; cf. Miller, 1956). The dotted line marks the theoretical human capacity for holding information in working memory: 2.5 bits. Accordingly, targets conveyed the same information for response selection across all tasks. In turn, gray gratings carried varying amounts of information for response selection in the switch, go/no-go, and oddball tasks. The information transmitted from stimuli to responses is derived from the notion of mutual information, $I(S; R)$, between sets of stimuli, $S = \{s_1, s_2, s_3, s_5, s_6\}$, and associated responses, $R = \{r_0, r_1, r_2\}$, in our three tasks (cf. Attneave, 1959; Koechlin & Summerfield, 2007; see details in supporting information).

information was transmitted only by "switch" gray Gabors, as these served as cues requiring anticipatory updating of episodic task rules. Note that these information estimates can be seen as a more formal and accurate way to translate into bits the mean probabilities of task events that are common practice in experimental psychology studies. Yet, bits provide a common metric to compare our manipulation of context across different task domains. For instance, instead of saying that a gray Gabor distractor occurs with an overall mean probability of $p = .08$ throughout our oddball task, we chose to quantify this in bits by saying that the sensory entropy of this distractor is $H(s_1) = -0.08 \cdot \log_2 0.08 = 0.29$ bits (cf. *x* axis of Figure 2). A similar formalism was used to quantify in bits the relative probabilities of specific sensorimotor processes, such as the joint probability of specific $s_i - r_j$ mappings using the concept of transmitted information: $I(s_i, r_j) = \log_2 p(s_i, r_j) - \log_2 p(s_i) - \log_2 p(r_2)$. For simplicity, additional sources of contextual information (i.e., stimulus-response congruency effects, stimulus repetition effects, etc.) were randomized and not modeled in these estimates. Figure 2 presents a summary of these information estimations, in line with the two specific predictions of our study; for a technical description, see supporting information and Cooper et al. (2016).

Behavioral Analyses

Reaction times (RTs) are reported from correct trial runs only, while trial runs containing any false alarm, omission, or other errors were discarded. Errors were used to compute accuracy indexes. Only the first three target trials following a gray grating entered the analyses, since behavioral costs typically reach an asymptote in later trials (Monsell, 2003). Restart costs were defined as the difference in mean RTs and errors between the first and second target responses following any gray grating. Equivalent indices were obtained for the two control tasks. Mixing costs were estimated for the switch task only as the difference in mean RTs and errors between third target responses in the switch versus go/no-go tasks. Third targets provided a relatively pure index of mixing costs independent from restart costs. Finally, although we did not expect to find switch-specific behavioral costs due to our long cue-to-target intervals (cf. Foxe, Murphy, & De Sanctis, 2014), local switch costs were also computed as the difference in mean RTs and errors between first target responses after switch versus repeat cues. Only color-rule trials were considered in the behavioral analyses of switch trials, to limit any task switch asymmetries. Mean RTs and percentage error trials were subjected to repeated measures analysis of variance (ANOVA) with the following factors: gray grating (vertical vs. horizontal), target trial (1st, 2nd, 3rd target in the trial run), and task context (oddball, go/no-go, switch). All participants had an overall hit rate better than 89% in the switch task, with at least 60% correct trial runs to the initial three targets following any gray Gabor (cf. Cooper et al., 2016). These strict selection criteria were meant to avoid post-error slowing effects, and ensured that participants had complied with task instructions.

EEG Recordings and ERP Analyses

Continuous EEG data (0.05–100 Hz band pass) were collected using SynAmps RT amplifiers (NeuroScan, TX) from 60 scalp sites using tin electrodes mounted on an elastic cap (Synamp2 Quikcap, Compumedics, TX) at a sampling rate of 500 Hz. EEG electrodes were placed following the extended 10–20 position system with a left mastoid reference, and later rereferenced offline to the algebraic average of the right and left mastoids. Four additional electrodes were placed above and below the left eye and on the outer canthi of both eyes to monitor blinks and eye movements. Sensor impedances were kept below 10 kΩ, as in Cooper et al. (2016).

EEG data were processed using MATLAB (Mathworks, Natick, MA) through a pipeline utilizing EEGLAB (Delorme & Makeig, 2004), CSD Toolbox (Kayser & Tenke, 2003), and in-house functions. Preprocessing was performed in EEGLAB as follows. EEG data were rereferenced offline to linked mastoids and band-pass filtered (0.1–30 Hz). Epochs for each stimulus type were extracted from −200 ms to +1,200 ms relative to stimulus onset, with a 200-ms prestimulus baseline. Trials with nonstereotyped artifacts (e.g., cable movement, swallowing) were removed, and stereotyped artifacts (e.g., blinks, eye movements) were deleted using independent component analysis (extended infomax algorithm; Bell &

Sejnowski, 1995). Note that only color-rule trials were considered for analysis of switch trials (to limit any influence of task asymmetries relative to the control tasks), which resulted in an average of 142.8 (± 9.6 *SD*) gray distractor, 73.5 (± 4.9) target1, and 75.3 (± 5.4) target3 trials for oddball; 126 (± 16) no-go, 130 (± 16) target1 and 122.2 (± 15.6) target3 go trials for go/no-go; and 28.4 (± 4.6) repeat cues, 30.7 (± 4.8) repeat target1 and 30.9 (± 4.8) repeat target3 trials; 31.4 (± 3.7) switch cues, 31.1 (± 3.7) switch target1 and 31.2 (± 3.6) switch target3 trials for the switch task. This same data set was employed to examine EEG oscillatory dynamics of task switching in the same sample of young participants (cf. Cooper et al., 2016).

Neighboring electrodes were combined into topographical regions of interest (ROIs) (frontopolar: Fp1, Fpz, Fp2; frontal: F1, Fz, F2; central: C1, Cz, C2; parietal: P1, Pz, P2) to preserve statistical power (Picton et al., 2000). Time windows for ERP analyses were selected based on visual inspection of the corresponding grand mean waveforms. Two groups of ERP measures were obtained—context-locked and target-locked—based on the assumption that gray gratings provided the temporal context for subsequent target detection. Thus, five distinct ERP components were measured and analyzed in the context-locked waveforms: P3 (350–400 ms), two windows of a late positive complex (LPC_1: 550–600 ms, LPC_2: 750–850 ms), and a frontally distributed slow negativity toward the end of the recording epoch (contingent negative variation, CNV; 1,000–1,200 ms). In the target-locked waveforms, maximal signal amplitudes were observed at one latency window: P3 (350–400 ms), and only for the first target following any gray grating, two more latency windows captured a sustained positivity (SP) starting around 300 ms posttarget onset and lasting to the end of the epoch (SP_1: 550–600 ms and SP_2: 750–850 ms). The latency of P300 potentials is known to vary with task complexity (Kappenman & Luck, 2012; Kutas, McCarthy, & Donchin, 1977), and hence switch positivities were examined using a wider (300–900 ms) latency window. Accordingly, our distinction between domain-general P3 and switch positivities relied on their distinct scalp topographies and sensitivity to experimental factors, rather than on any differences in peak latencies.

Mean ERP amplitudes were analyzed using repeated measures ANOVA to examine our manipulation of temporal and task contexts on domain-general P3s—common to all tasks while uninfluenced by task switching demands and switch positivities. Firstly, a temporal context (gray grating, target3) factor examined differences in P3-like amplitudes between infrequent and temporally unpredictable gray gratings, and temporally predictable third targets following those gray gratings. Secondly, and given the highly different P3-like task effects observed for gray gratings (i.e., context P3) and third targets (i.e., target P3), the task context factor was tested separately for context-locked and target-locked ERP waveforms. Thus, context-locked ERP waveforms were analyzed considering the following within-subject factors: task context (switch, go/no-go, oddball), gray grating (vertical, horizontal), and ROI (frontopolar, frontal, central, parietal). Target-locked ERP waveforms were analyzed with the within-subject factors task context (switch, go/no-go, oddball), gray grating (vertical, horizontal), target trial (target1, target3), and ROI (frontopolar, frontal, central, parietal). The Greenhouse-Geisser (GG) sphericity correction was applied as needed. Corrected p values are reported, but original degrees of freedom are kept for easier reading. A significance level of $p < .05$ was adopted for all main statistical analyses, and a Bonferroni-corrected threshold ($0.05/4 = p < .0125$) was used for multiple tests at the four midline regions.

Analyses of ERP Scalp Topographies

As in many past studies (Polich & Comerchero, 2003; Squires et al., 1975), to assess the effects of temporal and task contexts on ERP positivities, we examined the scalp distribution of mean amplitudes across four midline regions (frontopolar, frontal, central, parietal), two temporal contexts (gray grating, target3), and three task contexts (switch, go/no-go, oddball). Further, to identify switch P3-like positivities as distinct from domain-general P3, we looked for significant interactions with the gray grating factor (switch vs. repeat) in the switch task only. Next, to address our first and second hypotheses, we examined changes in the scalp distribution of domain-general P3 across the three task contexts, as well as for the two temporal contexts, namely, for proactive (gray gratings) and reactive (target3) processing modes, respectively. Accordingly, answers to our first and second hypotheses were addressed by looking for significant ANOVA interactions between the ROI factor and the temporal and task context factors, respectively. Further, we specifically tested the null hypothesis of similar scalp distributions for switch positivities and domain-general P3 by examining the interaction between ROI × ERP component in the switch task only. To minimize the effects of volume conduction on the analyses of scalp topographies and favor integration with past studies, data were also compared by using a surface Laplacian filter (smoothing = 10-5, number of iterations = 10, spherical spline order = 4; Kayser & Tenke, 2006; Urbach & Kutas, 2002).

Results

Behavioral Results

All three tasks were performed very efficiently, with an average of only 6.3% incorrect trials in the switch task (95% CI [5.1, 7.4]), 4.5% in the go/no-go (95% CI [3.5, 5.5]), and 0.4% in the oddball (95% CI [0.3, 0.5]). A main effect of task, $F(2,60) = 47.6$, $p < .0001$; GG = 0.83; $\eta^2 = .61$, confirmed differences in overall error rates among all three tasks (all $ps < .001$; Figure 3A). Accuracy did not vary across target trials in the oddball, but larger error rates were observed in first relative to second target trials following any gray gratings in both switch and go/no-go tasks (all $ps < .001$), with no further differences between second and third target trials, as revealed by a two-way interaction Task × Target trial, $F(2,120) = 5.1$, $p < .003$; GG = 0.73; $\eta^2 = .15$. The three-way interaction with gray grating was marginally significant, $F(4,120) = 2.72$, $p = .08$; GG = 0.52; $\eta^2 = .08$, pointing to significantly greater error rates to the first target trial following switch compared to repeat gray gratings in the switch task only (9.5% vs. 6.5% errors, respectively, $p < .02$), which confirmed the presence of local, restart, and mixing costs for accuracy data in the switch task. No other effects reached significance.

The speed of correct target responses differed among all tasks ($ps < .001$; Figure 3B), as revealed by a main task context effect, $F(2,60) = 99.9$, $p < .0001$; GG = 0.76; $\eta^2 = .77$. A two-way interaction Task context× Target trial, $F(4,120) = 17.8$, $p < .0001$; GG = 0.59; $\eta^2 = .37$, revealed the presence of restart costs in the switch and go/no-go tasks, both showing slower responses to the first than the second or third targets (all $ps < .001$), without any further slowing observed between the two latter trials. In contrast, the oddball task did not show any first trial slowing. Mixing costs were inferred from the larger mean RTs to third target trials in the switch compared to both control tasks (all $ps < .001$; Figure 3B). The third order interaction with gray grating failed to reach significance,

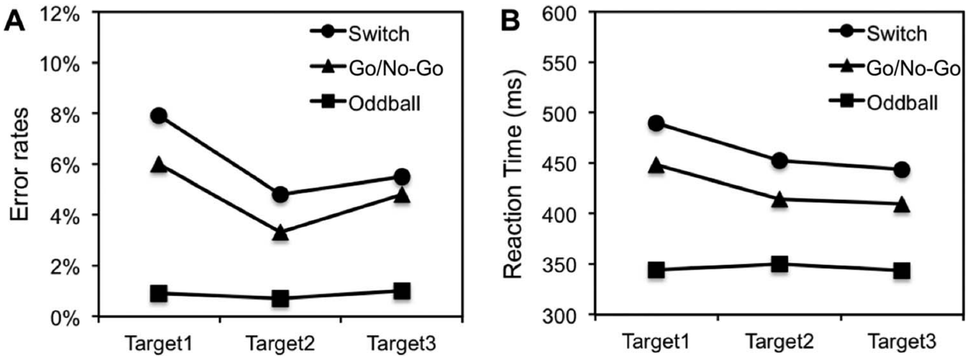

Figure 3. Behavioral results. Error rates and mean reaction times (RTs) to correct target trials as a function of target trial position following a gray grating in each of the three tasks. Residual restart and mixing costs were observed in both incorrect (left) and correct trials (right). Local (switch > repeat) costs were observed to the first target in incorrect trials only (not shown).

suggesting the absence of local switch costs in the mean RTs to correct first target trials in the switch task, an expected outcome given our long 1,900-ms cue-target intervals (cf. Foxe et al., 2014).

Electrophysiological Results

Figure 4 summarizes the grand ERP waveforms over midfrontal and midparietal regions to gray gratings, and to the first (target1) and third (target3) target trials across all tasks. Since ERPs to second target trials (not shown) present an intermediate stage, analyses focused on first and third target trials to maximize trial differences. Through visual inspection, three distinct ERP positivities could be identified in the context-locked ERP waveforms of the switch task, showing maximal amplitudes over centroparietal regions: P3 (350–400 ms), LPC$_1$ (550–600 ms), and LPC$_2$ (750–850 ms). These two aspects of the LPC best captured switch-related contextual effects. Finally, a sustained frontally distributed CNV-like negativity extended from circa 800 ms until the onset of

COLOR IN ONLINE AND PRINT

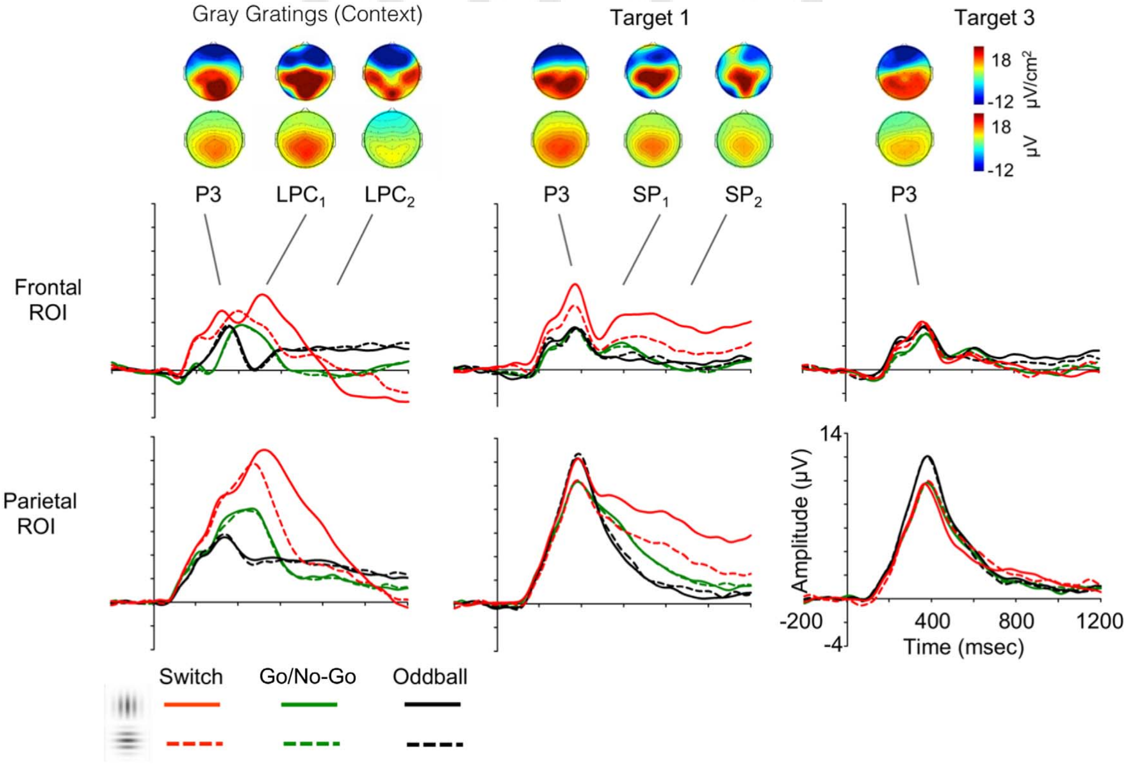

Figure 4. Grand-averaged ERPs. Brain responses are shown from midline frontal and parietal ROIs to vertical and horizontal gray gratings and to the first and third target gratings in the switch, go/no-go, and oddball tasks. The second target trial following gray gratings (not shown) also elicited a SP of lesser intensity to that of first target trials. Continuous lines: Trial runs starting with a switch gray grating in the switch task (vertical/horizontal grating orientation was counterbalanced across subjects). Dashed lines: Trial runs starting with a repeat gray grating in the switch task. The largest differences in the intensity of domain-general P3 and switch positivities occurred in response to gray gratings, as well as to the ensuing first target trials. Scalp topographies of mean amplitudes (μV) and surface Laplacian values (μV/cm^2) are shown for switch trials at three latency windows: 350–400 ms, 550–600 ms, and 750–800 ms.

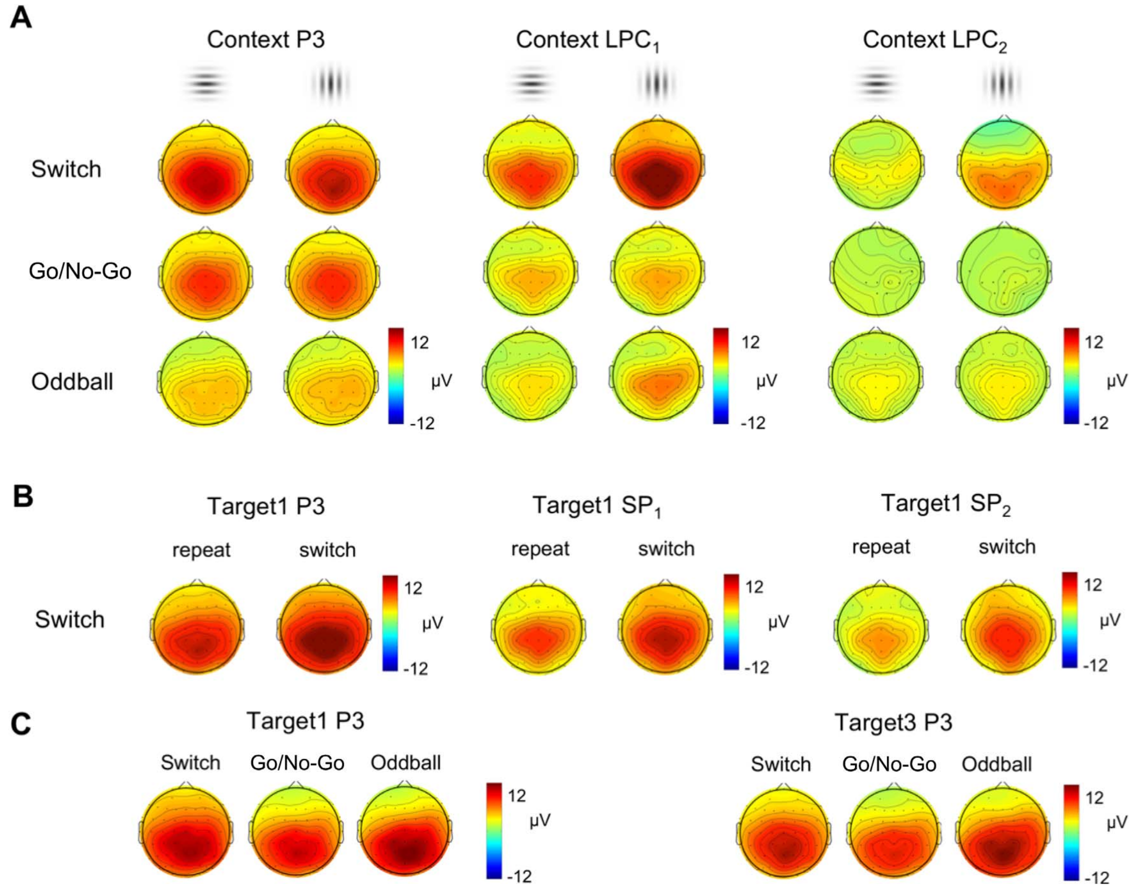

Figure 5. Scalp topography of domain-general P3 and switch P3-like positivities. A: Scalp distribution of mean voltages for context-locked P3, LPC_1, and LPC_2 positivities to horizontal (repeat) and vertical (switch) gray gratings across the three task domains. B: Scalp distribution of target-locked P3, SP_1, and SP_2 positivities to first target (target1) trials following repeat and switch gray gratings in the switch task. C: Scalp distribution of domain-general target P3 and LPC_1 positivities to third target (target3) trials across the three task domains.

the first target stimulus. A target P3 (350–400 ms) was present in the target-locked waveforms, with similar amplitudes and centro-parietal scalp distribution across all three task contexts, as shown in Figure 4 and 5. In addition, a SP starting 300 ms posttarget onset and lasting until the end of the recording epoch was observed to target1 in the switch and—to a lesser extent—also the go/no-go tasks. Modulations of these context- and target-locked ERP waveforms are described below. The visual P1 and N1 were not modulated by task conditions, and will not be discussed further.

Context Effects on Domain-General P3s

Two domain-general P3s with 350–400 ms peak latencies were present across all three tasks (labeled as "context P3" and "target P3" in Figure 4 and 5), and their mean amplitudes were not modulated by the gray grating factor in any of the three tasks. Instead, as reported below, these two P3s showed distinct scalp topographies and were differently modulated by temporal and task contexts, which justifies their consideration as two distinct P3 components.

As predicted by our model, both the temporal and task contexts modulated the intensity and scalp topography of domain-general P3s, as reflected by significant Temporal context× Task context, $F(2,60) = 17.6$, $p < .0001$; GG = 0.86; $\eta^2 = .37$, and Temporal context × Task context × ROI interactions, $F(6,180) = 35.5$, $p < .0001$; GG = 0.53; $\eta^2 = .54$. Given the very different P3-like modulations elicited by gray gratings and colored targets, Table 1 presents the relevant ANOVA results separately for context P3 and target3 P3. Firstly, increasing task demands elicited larger context P3 amplitudes, as revealed by a main task effect. Follow-up contrasts revealed a larger context P3 for the switch as compared to the other two tasks (all $ps < .005$), with no such differences between oddball and go/no-go tasks (Figure (4 and 5)A). A Task context× ROI interaction revealed that these larger context P3 amplitudes in the switch compared to the other two tasks occurred only at central and parietal regions (all $ps < .01$; Figure (4 and 5)A, 6A,C, left panels). In sharp contrast, mean target3 P3 amplitudes were larger in the oddball compared to the other two tasks, and only at the parietal region ($ps < .005$), as revealed by a significant Task context × ROI interaction (see Table 1; Figures 4, 5C, 6B,D).

Secondly, the significant interaction between temporal context and task context was further examined by comparing mean amplitudes of context P3 and target3 P3 in each task domain separately. Significantly larger target3 P3 than context P3 mean amplitudes were observed in the oddball and go/no-go tasks (main temporal context effect: $F(1,30) = 46.1$, $p < .0001$; $\eta^2 = .61$, and $F(1,30) = 7.7$, $p < .01$; $\eta^2 = .20$, respectively), with differences at central and parietal regions (Temporal context × ROI: $Fs(3,90) > 30.4$, $ps < .0001$; $\eta^2s > .52$). In contrast, the Temporal context × ROI interaction failed significance in the switch task, $F(3,90) = 1.4$, $p = .24$, suggesting no differences in mean P3 amplitudes elicited by gray gratings and third target trials in the switch task (Figure 6B,A left panel). This pattern of results was confirmed with surface

Table 1. *ANOVAs Showing Task Effects for Two Measures of Context P3 and Target3 P3*

		Amplitudes		Surface Laplacian	
	df	*F*	η^2	*F*	η^2
Context P3					
Task	2,60	6.2**	0.17	22.1***	0.42
Task × ROI	6,180	15.5***	0.34	13.9***	0.32
Target3 P3					
Task	2,60	2.48 *n.s.*	0.08	0.60 *n.s.*	0.02
Task × ROI	6,180	9.8***	0.25	4.2**	0.12

*$p < .05$. **$p < .01$. ***$p < .0001$.

Laplacian values (Table 1; Figure 6C,D left panel), which attest to different topographies with varying task demands for both context P3 and target3 P3. Thus, whereas target3 P3 showed a centroparietal maximum under the simplest oddball task, context P3 to the gray gratings showed maximal frontal intensities under the most difficult switch task (Figure 4).

Of note, mean target P3 amplitudes differed for target1 versus target3 trials, as suggested by a main trial effect, $F(1,30) = 10.4$, $p < .003$; $\eta^2 = .26$, but this was true only in the switch task, as revealed by a two-way Task context × Target trial interaction, $F(2,60) = 6.8$, $p < .003$; GG = 0.86; $\eta^2 = .18$. Simple tests of effects revealed that neither oddball nor go/no-go target P3 amplitudes changed from first to third target trials (see Figure 4, 5C). In contrast, target1 P3 in the switch task was larger than target3 P3 across all midline regions (all *p*s < .005), owing to an overlapping SP as described below.

Context Effects on Switch P3-Like Positivities

The gray grating factor yielded significant main effects and three-way interactions with task context and ROI for context-locked LPC_1, $F(6,180) = 9.5$, $p < .0001$; GG = 0.39; $\eta^2 = .24$, and LPC_2 positivities, $F(6,180) = 24.3$, $p < .0001$; GG = 0.38; $\eta^2 = .45$, as well as for the SP to the first target following a switch cue, $Fs(1,30) > 10.7$, $ps < .003$; $\eta^2\text{s} > .26$. In all cases, LPC_1 and LPC_2 amplitudes in the switch task were larger for switch than for repeat gray gratings over midcentral and midparietal regions (all *p*s < .01; Figure 7A), whereas only LPC_1 also differed among gray gratings over frontopolar and frontal regions (all *p*s < .02; Figure 4, 5, 7A). Mean amplitudes for the sustained positivity (SP_1 and SP_2) to target1 were largest for switch gray gratings across all midline regions (Figure 4, 5B, 7B). This effect was present already in the latency window of target1 P3 (gray grating main effect: $F(1,30) = 11.5$, $p < .002$; $\eta^2 = .28$), with differences at frontal, central, and parietal regions (all *p*s < .005; interaction Gray grating × ROI: $F(3,90) = 3.5$, $p < .04$; $\eta^2 = .11$).

In sum, two distinct switch-related positivities were apparent: a context-locked late positive complex (500–850 ms; described as a "switch positivity" by Karayanidis et al., 2009), and a sustained SP (300–1,200 ms) elicited by the first target (target1) following a switch cue (cf. Barceló et al., 2008).

Scalp Topography of Domain-General P3s Versus Switch Positivities

The main question of this study specifically required testing the null hypothesis of similar scalp distributions of switch positivities and domain-general P3s, as indicated by the absence of an interaction between ROI × ERP component. Thus, differences in the midline scalp distribution of P3-like amplitudes and Laplacian values were examined in response to switch gray gratings (Table 2, Figure 7A,C) and first switch target trials (Table 3, Figure 7B,D).

Firstly, significant differences in midline topographies of context P3 and two aspects of an LPC to the switch cues were revealed by two-way interactions between ERP and ROI for mean amplitudes and surface Laplacian values (Table 2; Figure 7A,C).

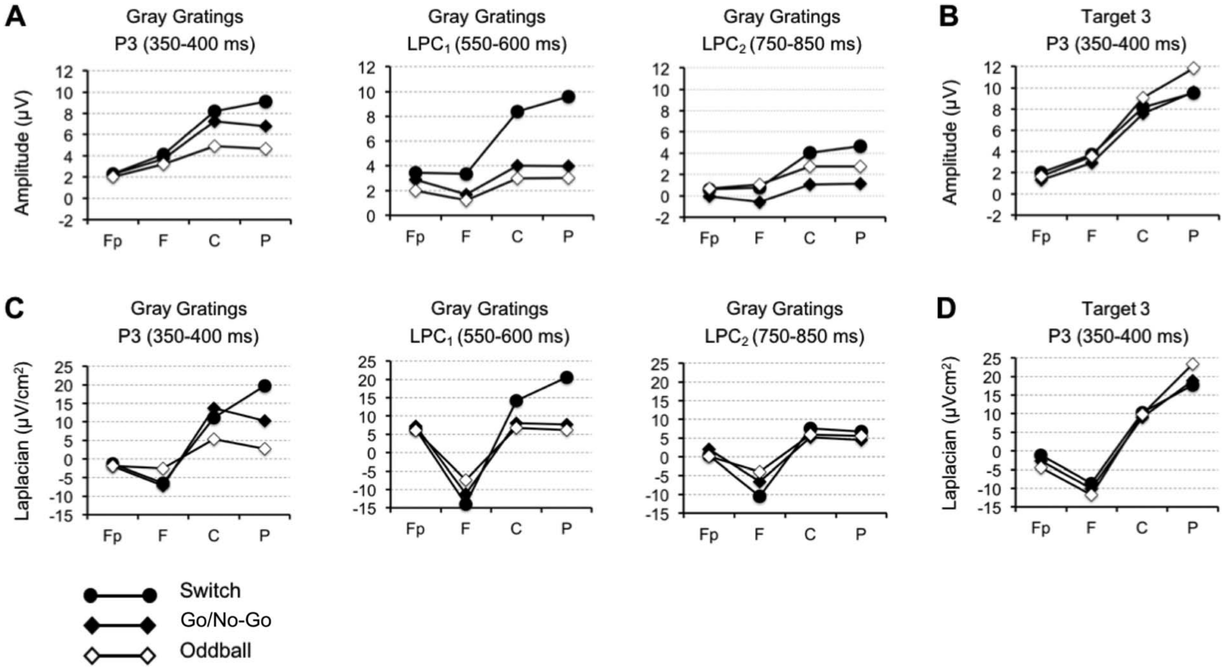

Figure 6. Topographic profiles of domain-general P3 and switch positivities across three task domains. A: Mean amplitudes of context P3 and the early (LPC_1) and late (LPC_2) aspects of a late positive complex (LPC) in response to gray gratings under different task demands. B: Mean amplitudes of target P3 in response to third target (target3) trials under different task demands. C, D: Surface Laplacian values for the same conditions as in (A) and (B).

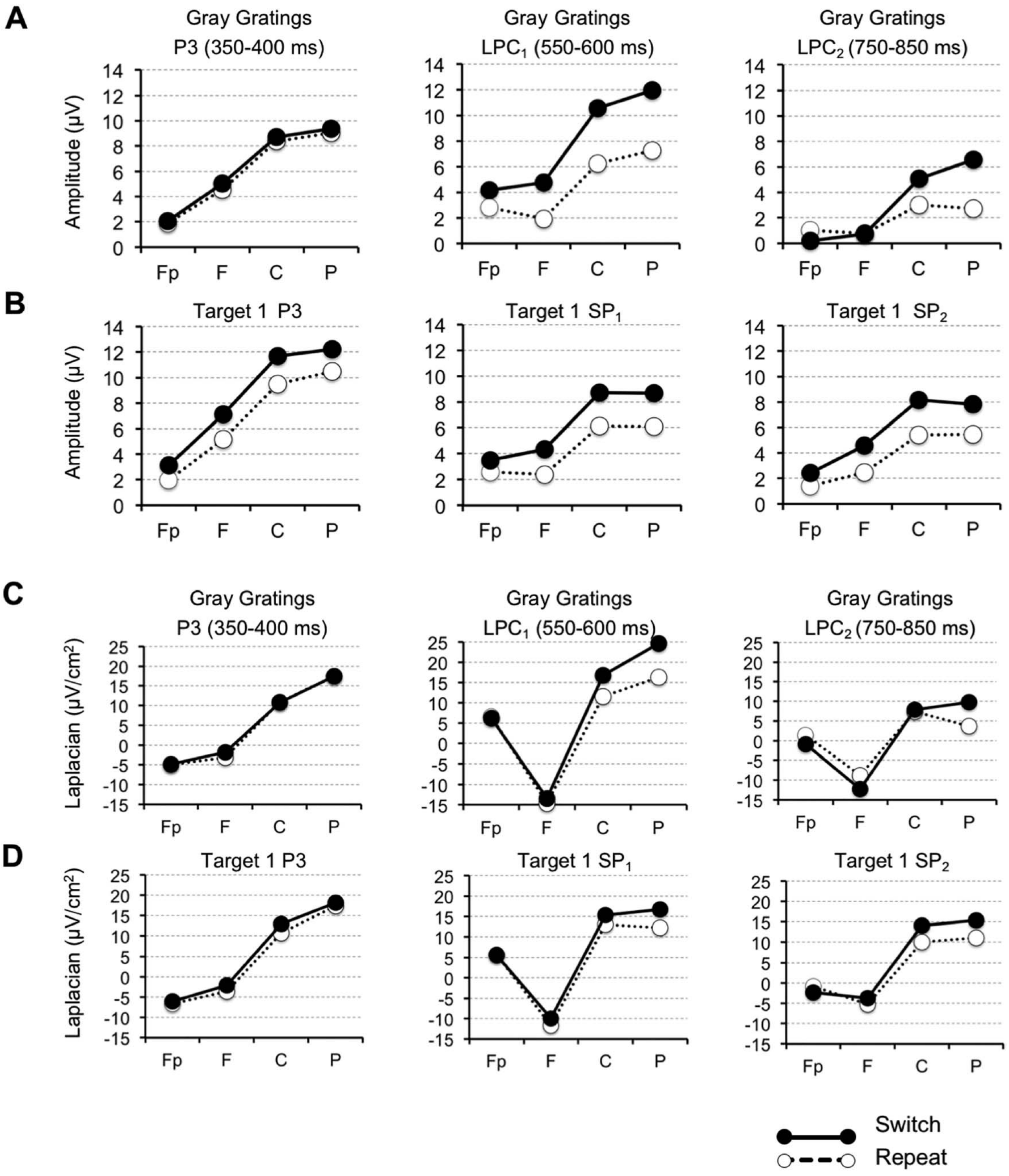

Figure 7. Topographic profiles of domain-general P3 and switch positivities for switch and repeat trials in the switch task. A: Mean amplitudes of context P3 and the early (LPC$_1$) and late (LPC$_2$) aspects of the late positive complex (LPC) in response to gray gratings prompting for a switch and repetition in task rules, respectively. B: Mean amplitudes of target P3 and the early (SP$_1$) and late (SP$_2$) aspects of the SP in response to first target trials following gray gratings prompting for a switch and repetition in task rules. C, D: Surface Laplacian values for the same conditions as in (A) and (B).

Table 2. *ANOVAs Comparing the Scalp Topographies of Context P3 and Two Aspects of the Late Positive Complex (LPC) in the Switch Task*

		Amplitudes				Surface Laplacian			
		LPC$_1$		LPC$_2$		LPC$_1$		LPC$_2$	
	df	*F*	η^2	*F*	η^2	*F*	η^2	*F*	η^2
Context P3 versus LPC									
ERP (P3 vs. LPC)	1, 30	13.4**	0.30	17.3***	0.37	10.8***	0.27	35.7***	0.54
ERP × ROI	3, 90	4.8*	0.13	9.3***	0.24	12.4***	0.29	8.6***	0.22

*$p < .05$. **$p < .01$. ***$p < .0001$.

Table 3. *ANOVAs Comparing the Scalp Topographies of Target1 P3 and Two Aspects of the Sustained Positivity (SP) in the Switch Task*

		Amplitudes				Surface Laplacian			
		SP_1		SP_2		SP_1		SP_2	
	df	*F*	η^2	*F*	η^2	*F*	η^2	*F*	η^2
Target1 P3 versus SP									
ERP (P3 vs. SP)	1, 30	13.2***	0.31	22.1***	0.42	0.01 *n.s.*	0.000	0.33 *n.s.*	0.011
ERP × ROI	3, 90	13.1***	0.30	21.1***	0.41	8.2***	0.22	2.65 *n.s.*	0.08

*$p < .05$. **$p < .01$. ***$p < .0001$.

Follow-up tests of effects revealed different topographies for P3 and LPC_1 (amplitudes: P3 < LPC_1 at all sites, all *ps* < .002, Figure 7A; Laplacian: P3 > LPC_1 at frontal; P3 < LPC_1 at central and parietal, all *ps* < .005; Figure 7C). Likewise, scalp topographies differed between P3 and LPC_2 (amplitudes: P3 > LPC_2 at all ROIs; all *ps* < 0.004, Figure 7A; Laplacian: P3 > LPC_2 at frontal, *p* < .002, Figure 7C).

Secondly, the scalp topography of target1 P3 and the early SP_1 and late SP_2 aspects of a SP to first switch targets also differed as revealed by two-way interactions between ERP and ROI for mean amplitudes and surface Laplacian values (Table 3; Figure 7B,D). Simple tests of effects showed different topographies between target1 P3 and SP_1 (amplitudes: P3 > SP_1 at all ROIs; all *ps* < .02, Figure 7B; Laplacian: P3 < SP_1 at frontopolar and P3 > SP_1 at frontal; *ps* < .001, Figure 7D). Topographies of target1 P3 and SP_2 differed for mean amplitudes: P3 > SP_2 at frontal, central, and parietal (all *ps* < .002, Figure 7B), but not for Laplacian values (Table 3; Figure 7D).

In sum, these analyses of scalp topographies resulted in significant ERP × ROI interactions when comparing domain-general P3s in the switch task with two switch P3-like positivities identified in the preceding analyses (Table 2, 3). These analyses failed to support the null hypothesis, thus disconfirming our original visual impression of apparently similar scalp topographies for switch P3-like and domain-general P3 potentials in the switch task (cf. Figure (4 and 5)). On the contrary, these analyses suggested significant—albeit subtle—split-second changes in the disposition of frontoparietal sources with varying contextual and task demands (see Figure 7; cf. Kappenman & Luck, 2012; Urbach & Kutas, 2002).

Linear Regression Analyses

Finally, to further assess the reliability of our model's predictions, we performed linear regression analyses using mean P3 and P3-like amplitudes from midfrontal and midparietal ROIs as criteria; predictors were the values of transmitted sensorimotor (S-R) information estimated for the six Gabor gratings used in each task (Figure 2; see Table S7 in supporting information). Given the very distinct P3-like modulations elicited by gray gratings and colored targets, regression analyses were performed separately for either temporal context. For a more sensitive analysis of this linear association, the same regression analyses were run separately for each subject, and *t* tests were used to examine whether the standardized (beta) regression weights averaged across all participants differed significantly from zero. The significance of mean beta regression weights across subjects is provided in brackets next to R^2 coefficients for the grand ERP averages. For the gray gratings, a direct association was found between increasing information and midparietal amplitudes for context P3 ($R^2 = .66$, $p = .05$; Figure 8A) [beta = .49, $t(30) = 6.12$; $p = .0001$], and context LPC_1 ($R^2 = .88$, $p = .008$; Figure 8A) [beta = .73, $t(30) = 11.8$; $p = .0001$], and midfrontal amplitudes for context LPC_1 ($R^2 = .92$, $p = .002$; not shown) [beta = .40, $t(30) = 3.8$; $p = .01$]. Of note, mean context LPC_2 amplitudes were not predicted by sensorimotor information either at parietal ($R^2 = .473$, $p = .13$; Figure 8A) [although this reached significance across subjects: beta = .34, $t(30) = 3.7$; $p = .01$] or frontal regions ($R^2 = .52$, $p = .11$) [beta = −.14, $t(30) = -1.39$; $p = .10$], reflecting that this switch P3-like component was present in the switch task only (cf. Figure (2 and 8)A). For the targets, an inverse relationship was apparent between increasing sensorimotor information and smaller target P3 amplitudes, although this did not reach significance either at parietal ($R^2 = .284$, $p = .28$; Figure 8B) [beta = −.09, $t(30) = -.82$; $p = .42$], or frontal regions ($R^2 = .445$, $p = .14$) [beta = .09, $t(30) = .83$; $p = .41$]. This is consistent with our model's predictions (Figure 2) in that the strongest modulations of P3-like positivities across tasks were linked to the processing of unexpected gray gratings rather than to target detection per se (cf. Posner & Petersen, 1990).

Discussion

This study addressed one important question for a theoretical integration of past P300 research on the hypothesis of context updating (Donchin, 1981) with newer ERP studies on the cognitive control of task switching, as hypothetically regulated by a common frontoparietal network of cortical regions. Our results provide new evidence about our main research question and two ancillary hypotheses about the relationship between domain-general P3s and switch P3-like positivities. Firstly, the results clearly support that switch positivities are functionally distinct from P3s recorded in simple oddball and go/no-go tasks, including subtle—albeit significant—changes in scalp topography. Secondly, our results support the hypothesis that the temporal context (i.e., proactive preparation vs. reactive execution of visuomotor rules) was a crucial determinant of the scalp distribution of both domain-general P3s and switch positivities. Finally, results also lent support to our second hypothesis that gradually larger frontoparietal P3-like positivities were elicited under higher cognitive demands, but only for those P3-like potentials elicited by temporarily surprising events that proactively prompted for future rule execution (Cooper et al., 2016; Kopp & Lange, 2013; Verleger et al., 2014).

These findings suggest that the present switch positivities are compatible with two types of context-updating mechanisms as defined by a model of cognitive control based on information theory: the updating of low-level sensorimotor S-R pathways (a

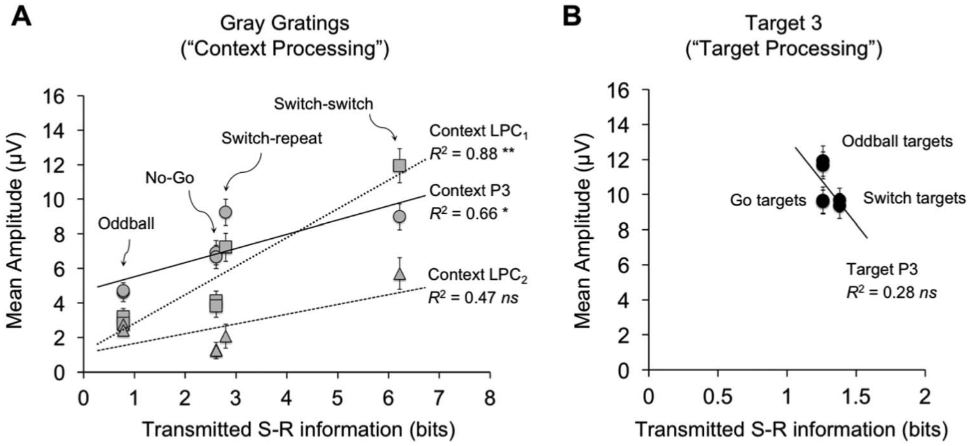

Figure 8. Linear regression of mean P3-like amplitudes against the amount of sensorimotor information transmitted by gray gratings (A) and the ensuing target3 gratings (B) across the three task contexts. Three functionally and topographically distinct P3-like components are modeled in response to the gray Gabor gratings: P3 (circles), LPC_1 (squares), and LPC_2 (triangles). Only one P3-like component is modeled in response to target Gabor gratings: P3 (black circles). In line with our model's predictions, only the switch task showed significant differences in mean P3-like amplitudes between vertical and horizontal gray gratings (i.e., switch-repeat vs. switch-switch cues).

domain-general mechanism common to many tasks), and the updating of higher-order task rules from episodic memory. When considered alongside domain-general P3s, the current results are compatible with the hypothesis of switch positivities as part of an extended P300 family of late positive potentials, and also as plausible neural indexes of a multiple demand system (Duncan, 2013) of frontoparietal generators being rapidly engaged under varying contextual demands. These findings carry far-reaching implications for a redefinition of the P300 component in terms of an extended family of late P3-like positivities involved in cognitive control.

Two Domain-General P3s Index Distinct Proactive and Reactive Control Modes

The present analyses identified two functionally distinct domain-general P3s: one context-locked P3 (350–400 ms) and one target-locked P3 (350–400 ms). These two ERP positivities were examined in their simplest form in response to the infrequent gray gratings and target gratings in the oddball task, respectively, although they were also clearly apparent in the go/no-go and switch tasks. These two domain-general P3s fit well with the two aspects of conventional P300 potentials, namely, an anterior P3a to rare distracters and a target P3b with its characteristic midparietal scalp distribution (Polich, 2007). However, these P3-like modulations cannot be explained by the updating of stimulus features alone, but are better accounted for in terms of sensorimotor S-R links and amount of task-set information held in memory while upholding, preparing, or executing goal-directed actions (Verleger et al., 2014). Mean amplitudes and surface Laplacian values of context P3 and target3 P3 were differently modulated by increasing task demands (Figure 4–6A,B). This is consistent with the extant literature that describes two functionally and topographically distinct P300 aspects, namely, novelty P3a and target P3b (Spencer et al., 1999; Squires et al., 1975), except that our formal operationalization of both temporal and task contexts allowed us a much richer and finer-grained functional characterization beyond the conventional ignore versus attend dichotomy.

Critically, third target trials elicited very similar ERP waveforms across all tasks, a paradoxical outcome given the intuitive differences in task difficulty also supported by behavioral results. However, this outcome concurs with our model's prediction that, on average, target gratings transmitted similar amounts of sensorimotor information for response selection in all three tasks (Figure 2). The only reliable difference affected mean target3 P3 amplitudes parietally, which were largest in the simplest oddball task. This effect is consistent with the reduced target P3b observed in relatively more complex tasks (Donchin, 1981), and is also compatible with carryover interference from competing S-R mappings that may result in reduced mean P3b amplitudes several trials after a task transition (Barceló et al., 2002). These findings suggest that target P3b—when disentangled from temporal unpredictability (oddballness)—reflects one type of reactive control shared across many task domains, such as the execution of simple $s_i - r_j$ pathways (i.e., press a button to designated targets; cf. Verleger et al., 2014).

The model accurately predicted contextual effects upon mean P3 amplitudes to the gray gratings (hence described as context P3) that were mostly sensitive to task differences in cognitive demands. Overall, context P3 showed a relatively more frontal scalp distribution for oddball gray gratings, and a relatively more parietal distribution for the most informative switch gray gratings. One critical aspect that might account for the functional dissociation between context P3 and target3 P3 is the need to uphold a motor response to unpredictable onset of gray gratings within a context of infrequent no-go responses in the go/no-go and switch tasks, which confer those stimuli with higher-order sensorimotor information relative to the gray gratings in the oddball task (cf. Verleger et al., 2014; see supporting information). Importantly, stimulus oddballness alone (i.e., the temporal unpredictability of gray gratings relative to the more predictable colored target gratings) cannot explain the present results. Instead, context P3 amplitudes captured the oddballness of specific S-R links involved in the strategic resolution of contextual uncertainty, as formally estimated in terms of low- and high-level sensorimotor control (Verleger et al., 2014). This contextual predictability hypothesis would agree with evidence that infrequent and unexpected distracters convey large amounts of information that may overshoot working memory capacity, thus eliciting novelty P3a with a more anterior scalp distribution (Barceló et al., 2006; cf. Kopp & Lange, 2013).

In sum, target3 P3 potentials suggest similar reactive control processes across all task domains, whereas switch positivities overlaying context P3 and target1 P3 potentials hint at distinct proactive and early reactive control operations across tasks (Rubinstein, Meyer, & Evans, 2001). This functional dissociation is consistent with the model's predictions, and with carryover effects due to the temporal contiguity between the highly informative gray gratings and the first targets, not only in the switch task (Monsell, 2003), but also in the simpler go/no-go task (Allport et al., 1994; Barceló et al., 2008).

An LPC Indexes Proactive Task Rule Updating

An LPC (circa 500–900 ms) with a centroparietal scalp distribution was elicited by gray gratings both in the go/no-go and switch tasks, and was sensitive to the spatial orientation of gray gratings (i.e., switch cues) in the switch task. Both the early LPC$_1$ and late LPC$_2$ aspects showed larger mean amplitudes for switch than repeat cues over centroparietal regions (Figure 7A,C, central and right panels). In line with previous results from task-cueing paradigms, this effect may reflect higher-order context-updating operations, such as memory uploading of new S-R mappings in preparation for upcoming targets that need to be classified with new rules. This could be seen as one type of proactive control operation, presumably one requiring episodic memory retrieval of task rules (Dayan, 2007), consistent with our model's predictions (see Table S5). Topographic profiles of early LPC$_1$ and late LPC$_2$ showed larger intensities for switch than repeat cues over centroparietal regions (Figure 7A, central and right panels). Further, subtle differences in the scalp topography of early LPC$_1$ and late LPC$_2$ pointed to their distinct roles in proactive rule updating. The early LPC$_1$ showed maximal frontal intensities in response to switch cues, with lesser centroparietal intensities for repeat and no-go gray gratings. In contrast, the late LPC$_2$ was elicited only by switch cues with a distinctly larger intensity over parietal regions, and a comparatively lesser frontal involvement (Figure 4, 7A,C, right panels). This functional and topographical dissociation portrays LPC$_1$ as a process shared by both task cues and no-go distracters (e.g., the stopping or inhibition of active s_i-r_j mappings), which is a prerequisite for subsequent rule updating, specifically indexed by the late LPC$_2$ aspect. Hence, LPC$_1$ cannot be regarded as a pure switch-specific positivity, given that it partly encoded lower-level sensorimotor control also shared by no-go and repeat gray gratings. All in all, LPC modulations matched well our information estimates for gray gratings in the switch and go/no-go tasks (Figure 2, 8; Table S7 in the supporting information), with an early LPC$_1$ aspect indexing a mixture of both low-level sensorimotor control and high-order task rule updating, followed by a late LPC$_2$ more specifically related to rule updating.

Switch LPC$_1$ and LPC$_2$ showed distinct scalp topographies, indicative of significant—albeit subtle—changes in the configuration of underlying sources relative to classic P3 potentials. In general, LPC amplitudes were larger over centroparietal regions with comparatively smaller intensities over frontal regions in the switch task. Toward the end of our long 1,200-ms cue-target interval, the switch LPC subsided and ERP waveforms for switch and repeat gray gratings did not differ over parietal regions (Figure 4), which suggests that proactive rule updating was fully completed by the onset of the first target trial. This could explain the absence of local switch costs in the mean RTs of correct trials (cf. Kang, Diraddo, Logan, & Woodman, 2014), and it concurs with findings about a transient and short-lived signature of anticipatory task-set reconfiguration (Barceló et al., 2008; Kang et al., 2014; Karayanidis et al., 2011; Lavric et al., 2008). Regression analyses suggested a positive association between the amount of transmitted sensorimotor information and mean LPC$_1$ amplitudes over frontal and parietal regions, with gray gratings that overshot memory capacity eliciting larger LPC$_1$ amplitudes over frontal regions (Figure 8). This association might explain the presence of restart costs in first target trials following no-go distracters and repeat cues. In sum, these findings suggest context-locked LPCs are a mixture of functionally distinct neural operations, probably reflecting higher-order context-updating operations (i.e., proactive rule updating) necessarily more complex to those indexed by conventional P300 potentials to rare oddballs.

A Sustained Positivity Indexes Early Reactive Task Rule Implementation

A SP was elicited by first targets following any gray gratings in the switch and go/no-go tasks—but not in the oddball task (Figure 4). This SP was absent from third target trials, and has received little attention in past task-cueing studies. Two sources of evidence suggest that the SP to first targets may reflect carryover of residual interference from the previous gray grating. Firstly, the SP was observed only in first targets ensuing highly informative gray gratings, and those that overshot the theoretical human capacity for holding information in memory (2.5 bits in Figure 2; Miller, 1956). Secondly, task differences in the amplitude of this SP mimicked the information value and P3-like activity evoked by gray gratings (cf. Figure 2, 4, 5B).

In the switch task, the SP probably reflects additional reactive control during the first implementation of a simple visuomotor rule (Rubinstein et al., 2001). The mean amplitude of the SP to first targets was significantly larger following switch than repeat gray gratings, thus providing an electrophysiological index of local switch costs at target onset (Figure 7B), even though this did not translate into significantly longer RTs to correct first targets after a switch cue, probably owing to our long cue-to-target intervals. Instead, the larger error rates observed following switch than repeat cues suggest that this SP could somehow interfere with efficient rule execution on first target trials (Rubinstein et al., 2001). Further research is needed to clarify this dissociation between behavioral and electrophysiological indexes of local switch costs.

Finally, a large portion of residual behavioral costs, the mixing cost, was not captured by transient ERP waveforms to third target trials. Nevertheless, one might expect this mixing cost to be reflected in indexes of enduring neural activity sensitive to the overall amount of task-set information, $\Sigma(s_ir_j)$, held in working memory during the task. This post hoc hypothesis warrants further examination using further indices of sustained neural activity, as well as through a finer-grained parametrical manipulation of the total amount of task-set information.

Limitations and Future Challenges

There are a number of limitations in our attempt to model P3-like positivities from an information theory approach. Firstly, even though the largest differences in the amplitudes of context-locked ERP positivities appeared over centroparietal regions, our model predicted gradually more frontal activations with increasing task demands (Koechlin & Summerfield, 2007). However, this frontal displacement might be partly hidden by overlapping frontal negativities in our young adults (Figure 4, upper row), which suggests that formal models need to take into account individual differences in age and behavioral efficiency. Instead, our information estimates were done for an ideal subject with 100% correct responses, which is a good approximation given the high accuracy of our young participants in all tasks. Secondly, our information metrics did not consider some sources of contextual effects that may also modulate ERP positivities such as trial-by-trial perceptual and motor priming effects, or S-R spatial compatibility (Simon) effects. More fine-grained analyses are warranted to decide the contribution from additional contextual demands to those late ERP positivities. This aim could be achieved through a systematic parametrization of low- and higher-order sensorimotor control processes, for instance, by varying the number of response alternatives, the number of task rules, or the entropy of stimuli and responses (Barceló & Knight, 2007; Barceló et al., 2008; Kopp & Lange, 2013). Thirdly, our long interstimulus intervals favored a temporal segregation of ERP positivities. However, shorter intervals will likely result in a greater overlap between domain-general P3s and switch P3-like positivities (Karayanidis et al., 2003; Lavric et al., 2008; Nicholson et al., 2005). Moreover, time constraints are a crucial determinant of behavioral costs (Monsell, 2003), and they should be incorporated in more sophisticated formal models of cognitive control. Finally, conventional analyses of mean amplitudes at the sensor space were preferred to favor integration with the extant literature. However, the relative implication of specific nodes within the frontoparietal network will require more sophisticated procedures for identification of underlying ERP components, such as source localization, time-frequency decomposition (Cooper et al., 2016; Kappenman & Luck, 2012), and independent component analyses (Enriquez-Geppert & Barceló, 2016; Makeig et al., 1999).

Conclusions

The scalp topographies of two domain-general P3s (350–400 ms) differed significantly from the scalp topography of later switch P3-like positivities (500–900 ms) during both proactive and reactive control of task switching. A strict interpretation of this outcome points to distinct configurations of underlying sources for conventional P300 potentials elicited by infrequent oddballs (Spencer et al., 1999; Squires et al., 1975), as compared to late P3-like potentials observed in task switching (Barceló et al., 2006; Karayanidis et al., 2003). However, direct visual inspection of scalp topographies shown in Figure 5 suggests that all those P3-like positivities are still compatible with an extended family of P300 potentials with subtly distinct configuration of sources as a function of gradually more complex cognitive demands. Importantly, the largest modulations in this family of P300 potentials were observed during context updating in response to temporarily surprising gray gratings and in anticipation of target onset (cf. Petersen & Posner, 2012; Posner & Petersen, 1990). After all, it would be reasonable that a putative brain index of context updating engaged correspondingly more complex neural machinery to update higher-order representations of task-set information (cf. Barceló & Knight, 2007).

In spite of fine-grained topographic differences with domain-general P3s, the observed switch positivities showed a centroparietal scalp distribution compatible with an extended family of P3-like potentials observed across many task domains (i.e., attention, memory, language, decision making, etc). Indeed, switch positivities evoke an LPC that has long been associated with the classic P300 in terms of its latency, centroparietal scalp distribution, and response to experimental variables (Kappenman & Luck, 2012; Polich, 2007). In fact, few authors attempt a fine-grained topographical analysis to verify the nature of P300 potentials recorded in a variety of task domains (Holig & Berti, 2010). From this perspective, the P300 cannot be regarded as a single ERP component—*sensu strictu* it has never been such a thing. Instead, it might well correspond with the electrophysiological signature of a multiple demand system for the integration of contextually relevant information in a wide variety of cognitive domains (cf. Duncan, 2013). The frontoparietal scalp topography and intensity of this extended family of P3-like potentials critically depends on the temporal context for goal-directed behavior (i.e., proactive vs. reactive control modes; Braver, 2012), as well as on a hierarchy of low- and higher-order sensorimotor demands that can be finely operationalized with more formal models of cognitive control (Koechlin & Summerfield, 2007).

References

Allport, A., Styles, E. A., & Hsieh, S. (1994). Shifting intentional set: Exploring the dynamic control of tasks. In C. Umiltà & M. Moscovitch (Eds.), *Attention and performance XV: Conscious and nonconscious information processing* (pp. 421–452). Cambridge, MA: MIT Press.

Attneave, F. (1959). *Applications of information theory to psychology: A summary of basic concepts, methods and results*. New York, NY: Holt, Rinehart and Winston.

Barceló, F., Escera, C., Corral, M. J., & Periáñez, J. A. (2006). Task switching and novelty processing activate a common neural network for cognitive control. *Journal of Cognitive Neuroscience*, *18*(10), 1734–1748. doi: 10.1162/jocn.2006.18.10.1734

Barceló, F., & Knight, R. T. (2007). An information-theoretical approach to contextual processing in the human brain: Evidence from prefrontal lesions. *Cerebral Cortex*, *17*(Suppl 1), 51–60. doi: 10.1093/cercor/bhm111

Barceló, F., Periáñez, J. A., & Knight, R. T. (2002). Think differently: A brain orienting response to task novelty. *NeuroReport*, *13*(15), 1887–1892. doi: 10.1097/00001756-200210280-00011

Barceló, F., Periáñez, J. A., & Nyhus, E. (2008). An information theoretical approach to task-switching: Evidence from cognitive brain potentials in humans. *Frontiers in Human Neuroscience*, *1*, 13. doi: 10.3389/neuro.09.013.2007

Bell, A. J., & Sejnowski, T. J. (1995). An information-maximization approach to blind separation and blind deconvolution. *Neural Computation*, *7*(6), 1129–1159. doi: 10.1162/neco.1995.7.6.1129

Bledowski, C., Prvulovic, D., Hoechstetter, K., Scherg, M., Wibral, M., Goebel, R., & Linden, D. E. (2004). Localizing P300 generators in visual target and distractor processing: A combined event-related potential and functional magnetic resonance imaging study. *Journal of Neuroscience*, *24*(42), 9353–9360. doi: 10.1523/JNEUROSCI.1897-04.2004

Braver, T. S. (2012). The variable nature of cognitive control: A dual mechanisms framework. *Trends in Cognitive Sciences*, *16*(2), 106–113. doi: 10.1016/j.tics.2011.12.010

Cole, M. W., Reynolds, J. R., Power, J. D., Repovs, G., Anticevic, A., & Braver, T. S. (2013). Multi-task connectivity reveals flexible hubs for adaptive task control. *Nature Neuroscience*, *16*(9), 1348–1355. doi: 10.1038/nn.3470

Cooper, P. S., Darriba, A., Karayanidis, F., & Barceló, F. (2016). Contextually sensitive power changes across multiple frequency bands underpin cognitive control. *NeuroImage*, *132*, 499–511. doi: 10.1016/j.neuroimage.2016.03.010

Cooper, P. S., Garrett, P. M., Rennie, J. L., & Karayanidis, F. (2015). Task uncertainty can account for mixing and switch costs in task-switching. *PLOS ONE*, *10*: e0131556. doi: 10.1371/journal.pone.0131556

Dayan, P. (2007). Bilinearity, rules, and prefrontal cortex. *Frontiers in Computational Neuroscience*, *1*, 1. doi: 10.3389/neuro.10.001.2007

Delorme, A., & Makeig, S. (2004). EEGLAB: An open source toolbox for analysis of single-trial EEG dynamics including independent component analysis. *Journal of Neuroscience Methods*, *134*(1), 9–21. doi: 10.1016/j.jneumeth.2003.10.009

Donchin, E. (1981). Surprise! … Surprise? *Psychophysiology*, *18*, 493–513. doi: 10.1111/j.1469-8986.1981.tb01815.x

Duncan, J. (2013). The structure of cognition: Attentional episodes in mind and brain. *Neuron*, *80*(1), 35–50. doi: 10.1016/j.neuron.2013.09.015

Enriquez-Geppert, S., & Barceló, F. (2016). Multisubject decomposition of event-related positivities in cognitive control: Tackling age-related changes in reactive control. *Brain Topography*, Advance online publication. doi: 10.1007/s10548-016-0512-4

Foxe, J. J., Murphy, J. W., & De Sanctis, P. (2014). Throwing out the rules: Anticipatory alpha-band oscillatory attention mechanisms during task-set reconfigurations. *European Journal of Neuroscience*, *39*(11), 1960–1972. doi: 10.1111/ejn.12577

Fuster, J. M. (2001). The prefrontal cortex—An update: time is of the essence. *Neuron*, *30*(2), 319–333. doi: 10.1016/S0896-6273(01)00285-9

Holig, C., & Berti, S. (2010). To switch or not to switch: Brain potential indices of attentional control after task-relevant and task-irrelevant changes of stimulus features. *Brain Research*, *1345*, 164–175. doi: 10.1016/j.brainres.2010.05.047

Kang, M. S., Diraddo, A., Logan, G. D., & Woodman, G. F. (2014). Electrophysiological evidence for preparatory reconfiguration before voluntary task switches but not cued task switches. *Psychonomic Bulletin & Review*, *21*(2), 454–461. doi: 10.3758/s13423-013-0499-8

Kappenman, E. S., & Luck, S. J. (2012). ERP waveforms: The ups and downs of brainwave recordings. In S. J. Luck & E. S. Kappenman (Eds.), *The Oxford handbook of event-related potential components* (pp. 3–30). New York, NY: Oxford University Press.

Karayanidis, F., Coltheart, M., Michie, P. T., & Murphy, K. (2003). Electrophysiological correlates of anticipatory and poststimulus components of task switching. *Psychophysiology*, *40*(3), 329–348. doi: 10.1111/1469-8986.00037

Karayanidis, F., Mansfield, E. L., Galloway, K. L., Smith, J. L., Provost, A., & Heathcote, A. (2009). Anticipatory reconfiguration elicited by fully and partially informative cues that validly predict a switch in task. *Cognitive, Affective, and Behavioral Neuroscience*, *9*(2), 202–215. doi: 10.3758/CABN.9.2.202

Karayanidis, F., Provost, A., Brown, S., Paton, B., & Heathcote, A. (2011). Switch-specific and general preparation map onto different ERP components in a task-switching paradigm. *Psychophysiology*, *48*(4), 559–568. doi: 10.1111/j.1469-8986.2010.01115.x

Kayser, J., & Tenke, C. E. (2003). Optimizing PCA methodology for ERP component identification and measurement: Theoretical rationale and empirical evaluation. *Clinical Neurophysiology*, *114*, 2307–2325. doi: 10.1016/S1388-2457(03)00241-4

Kayser, J., & Tenke, C. E. (2006). Principal components analysis of Laplacian waveforms as a generic method for identifying ERP generator patterns: I. Evaluation with auditory oddball tasks. *Clinical Neurophysiology*, *117*(2), 348–368. doi: 10.1016/j.clinph.2005.08.034

Kieffaber, P. D., & Hetrick, W. P. (2005). Event-related potential correlates of task switching and switch costs. *Psychophysiology*, *42*(1), 56–71. doi: 10.1111/j.1469-8986.2005.00262.x

Koechlin, E., & Summerfield, C. (2007). An information theoretical approach to prefrontal executive function. *Trends in Cognitive Sciences*, *11*(6), 229–235. doi: 10.1016/j.tics.2007.04.005

Kopp, B., & Lange, F. (2013). Electrophysiological indicators of surprise and entropy in dynamic task-switching environments. *Frontiers in Human Neuroscience*, *7*, 300. doi: 10.3389/fnhum.2013.00300

Kutas, M., McCarthy, G., & Donchin, E. (1977). Augmenting mental chronometry: The P300 as a measure of stimulus evaluation time. *Science*, *197*(4305), 792–795. doi: 10.1126/science.887923

Lavric, A., Mizon, G. A., & Monsell, S. (2008). Neurophysiological signature of effective anticipatory task-set control: A task-switching investigation. *European Journal of Neuroscience*, *28*(5), 1016–1029. doi: 10.1111/j.1460-9568.2008.06372.x

Makeig, S., Westerfield, M., Jung, T.-P., Covington, J., Townsend, J., Sejnowski, T. J., & Courchesne, E. (1999). Functionally independent components of the late positive event-related potential during visual spatial attention. *Journal of Neuroscience*, *19*(7), 2665–2680.

Miller, G. A. (1956). The magical number seven plus or minus two: Some limits on our capacity for processing information. *Psychological Review*, *63*(2), 81–97. doi: 10.1037/h0043158

Monsell, S. (2003). Task switching. *Trends in Cognitive Sciences*, *7*(3), 134–140. doi: 10.1016/S1364-6613(03)00028-7

Nicholson, R., Karayanidis, F., Poboka, D., Heathcote, A., & Michie, P. T. (2005). Electrophysiological correlates of anticipatory task-switching processes. *Psychophysiology*, *42*(5), 540–554. doi: 10.1111/j.1469-8986.2005.00350.x

Petersen, S. E., & Posner, M. I. (2012). The attention system of the human brain: 20 years after. *Annual Review of Neuroscience*, *35*, 73–89. doi: 10.1146/annurev-neuro-062111-150525

Picton, T. W., Bentin, S., Berg, P., Donchin, E., Hillyard, S. A., Johnson, R., Jr., . . . Taylor, M. J. (2000). Guidelines for using human event-related potentials to study cognition: recording standards and publication criteria. *Psychophysiology*, *37*(2), 127–152. doi: 10.1111/1469-8986.3720127

Polich, J. (2007). Updating P300: An integrative theory of P3a and P3b. *Clinical Neurophysiology*, *118*(10), 2128–2148. doi: 10.1016/j.clinph.2007.04.019

Polich, J., & Comerchero, M. D. (2003). P3a from visual stimuli: Typicality, task, and topography. *Brain Topography*, *15*(3), 141–152. doi: 10.1023/A:1022637732495

Posner, M. I., & Petersen, S. E. (1990). The attention system of the human brain. *Annual Review of Neuroscience*, *13*, 25–42. doi: 10.1146/annurev.ne.13.030190.000325

Rubinstein, J. S., Meyer, D. E., & Evans, J. E. (2001). Executive control of cognitive processes in task switching. *Journal of Experimental Psychology: Human Perception and Performance*, *27*(4), 763–797.

Rushworth, M. F., Passingham, R. E., & Nobre, A. C. (2002). Components of switching intentional set. *Journal of Cognitive Neuroscience*, *14*(8), 1139–1150. doi: 10.1162/089892902760807159

Spencer, K. M., Dien, J., & Donchin, E. (1999). A componential analysis of the ERP elicited by novel events using a dense electrode array. *Psychophysiology*, *36*(3), 409–414. doi: 10.1017/S0048577299981180

Squires, N. K., Squires, K. C., & Hillyard, S. A. (1975). Two varieties of long-latency positive waves evoked by unpredictable auditory stimuli in man. *Electroencephalography and Clinical Neurophysiology*, *38*, 387–401. doi: 10.1016/0013-4694(75)90263-1

Urbach, T. P., & Kutas, M. (2002). The intractability of scaling scalp distributions to infer neuroelectric sources. *Psychophysiology*, *39*(6), 791–808. doi: 10.1111/1469-8986.3960791

Verleger, R., Baur, N., Metzner, M. F., & Smigasiewicz, K. (2014). The hard oddball: Effects of difficult response selection on stimulus-related P3 and on response-related negative potentials. *Psychophysiology*, *51*, 1089–1100. doi: 10.1111/j.1469-8986.2012.01408.x

Verleger, R., Jaskowski, P., & Wäscher, E. (2005). Evidence for an integrative role of P3b in linking reaction to perception. *Journal of Psychophysiology*, *19*, 165–181. doi: 10.1027/0269-8803.19.3.165

(Received October 15, 2015; Accepted November 23, 2016)

Supporting Information

Additional Supporting Information may be found in the online version of this article.

Table S1: Estimates of stimulus entropy and surprise in all tasks.

Table S2: Estimates of response entropy and surprise in the oddball task.

Table S3: Estimates of response entropy and surprise in the go/no-go and switch tasks.

Table S4: Estimates of transmitted sensorimotor (*s-r*) information in the oddball task.

Table S5: Estimates of transmitted sensorimotor (*s-r*) information in the go/no-go and switch tasks.

Table S6: Estimates of transmitted information between stimulus units and task-set units in the switch task.

Table S7: Summary of numerical values of transmitted information plotted in Figure 2.

Supplementary Material

Barceló and Cooper (in press, Psychophysiology)

Information theoretic estimations of sensory, motor, and sensorimotor control at two levels of a putative hierarchy of cognitive control for the switch, go/no-go and oddball tasks (cf., Attneave, 1959; Barceló et al., 2008; Koechlin & Summerfield, 2007; Miller, 1956).

Stimulus Entropy: $H(s_i) = -\Sigma_{i=1}^{6}\, p(s_i) \cdot \log_2 p(s_i)$

The same set and sequence of stimuli were used in all three tasks, and therefore, the same stimulus entropy can be assumed for all tasks, as shown in Table S1.

Table S1. Estimates of stimulus entropy and surprise in all tasks. Visual displays, stimulus codes, stimulus entropies, mean stimulus probabilities, and information surprise for the set of six Gabor stimuli used in all tasks.

Gabors	*S*[1]	*H*(*s*)	*p*(*s*)	$-\log_2 \cdot p(s)$
	s_1	0.29	0.08	3.64
	s_2	0.29	0.08	3.64
	s_3	0.47	0.21	2.25
	s_4	0.47	0.21	2.25
	s_5	0.47	0.21	2.25
	s_6	0.47	0.21	2.25
	$\Sigma H(s_i)=$	2.46		

Response Entropy: $H(r_j) = -\Sigma_0^j p(r_j) \cdot \log_2 p(r_j)$

The oddball task required one-button responses (r_1) and the absence of response (r_0) to all non-targets, hence the response set can be defined as $\boldsymbol{R} = \{r_0, r_1\}$, and response entropy can be estimated for the oddball task, as shown in Table S2.

Table S2. Estimates of response entropy and surprise in the oddball task. Response codes, response entropies, mean response probabilities, and information surprise for the set of responses used in the oddball task.

R	*H*(r)	*p*(r)	$-\log_2 \cdot p(r)$
r_0	0.45	0.58	0.78
r_1	0.53	0.42	1.26
$\Sigma H(r_i)=$	0.98		

---

[1] For simplicity, these estimates assume a stimulus set $\{S\}$ with only six stimuli, regardless of the fact that each Gabor grating was randomly displayed either to the left or the right visual hemifields.

The go/no-go and switch tasks required two-button responses (r_1, r_2) and the absence of response (r_0) to the grey gratings. Hence, the response set can be defined as $\boldsymbol{R} = \{r_0, r_1, r_2\}$, and estimates of response entropy for the go/no-go and switch tasks are shown in Table S3.

Table S3. Estimates of response entropy and surprise in the go/no-go and switch tasks. Response codes, response entropies, mean response probabilities, and information surprise for the set of responses used in the go/no-go and switch tasks.

R	$H(\mathrm{r})$	$p(\mathrm{r})$	$-\log_2 \cdot p(r)$
r_0	0.43	0.16	2.60
r_1	0.53	0.42	1.26
r_2	0.53	0.42	1.26
$\Sigma \mathrm{H}(r_i)=$	1.49		

Sensorimotor Information: $I(s_i, r_j) = \log_2 p(s_i, r_j) - \log_2 p(s_i) - \log_2 p(r_j)$

The information transmitted from stimuli to responses, $I(s_i, r_j)$, is derived from the notion of mutual information between sets of stimuli $\{S\}$ and responses $\{R\}$ (Attneave, 1959):

$$I(S;R) = \sum_i \sum_j p(s_i, r_j) \log \frac{p(s_i, r_j)}{p(s_i) p(r_j)}$$

The oddball task required one-button responses (r_1) only to the red Gabor gratings (s_5, s_6), and hence, low-level sensorimotor control for the relevant task-set units (s_i-r_j) can be estimated as shown in Table S4.

Table S4. Estimates of transmitted sensorimotor (s-r) information in the oddball task. Codes for hypothetical unitary S-R pathways, mean stimulus and response probabilities, joint s-r probabilities, and transmitted s-r information.

S-R	$p(s_i)$	$p(r_j)$	$p(s_i, r_j)$	$I(s_i, r_j)$
s_1-r_0	0.08	0.58	0.08	0.78
s_2-r_0	0.08	0.58	0.08	0.78
s_3-r_0	0.21	0.58	0.21	0.78
s_4-r_0	0.21	0.58	0.21	0.78
s_5-r_1	0.21	0.42	0.21	1.26
s_6-r_1	0.21	0.42	0.21	1.26

$\Sigma(s_i r_j) = 5.64$

The go/no-go and switch tasks required two-button responses (r_1, r_2) to classify blue and red Gabor gratings (s_3, s_4, s_5, s_6), and hence, estimates of low-level sensorimotor control for the relevant task-set units (s_i-r_j) when sorting by either color or form rules are shown in Table S5.

Table S5. Estimates of transmitted sensorimotor (s-r) information in the go/no-go and switch[2] *tasks.* Codes for hypothetical unitary S-R pathways, mean stimulus and response probabilities, joint s-r probabilities, and transmitted s-r information.

S-R	$p(s_i)$	$p(r_j)$	$p(s_i, r_j)$	$I(s_i, r_j)$
s_1-r_0	0.08	0.16	0.08	2.61
s_2-r_0	0.08	0.16	0.08	2.61
s_3-r_1	0.21	0.42	0.21	1.26
s_4-r_1	0.21	0.42	0.21	1.26
s_5-r_2	0.21	0.42	0.21	1.26
s_6-r_2	0.21	0.42	0.21	1.26
				$\Sigma(s_i r_j)= 10.26$

Episodic Information: $I(s_i, ts_k) = \log_2 p(s_i, ts_k\ ) - \log_2 p(s_i) - \log_2 p(ts_k)$

Only the switch task required access to episodic task-set (ts_1) information on just 8% of all trials (s_1-ts_1), while no task-set access (ts_0) was required in the remaining trials. Thus, the transmitted information between sensory stimuli and access to episodic memories in the switch task can be estimated as shown in Table S6.

Table S6. Estimates of transmitted information between stimulus units and task-set units in the switch task. Codes for hypothetical links between stimulus and task-set units, mean stimulus and task-set probabilities, joint s-ts probabilities, and transmitted episodic information for the switch task.

---

[2] Sensorimotor information in the switch task was slightly (~ 1 bit) larger for those color gratings that afforded bivalent responses (i.e., different buttons for either rule). For simplicity this additional source of contextual information was not included here.

$S\text{-}TS$	$p(s_i)$	$p(ts_k)$	$p(s_i, ts_k)$	$I(s_i, ts_k)$
$s_1\text{-}ts_1$	0.08	0.08	0.08	3.61
$s_2\text{-}ts_0$	0.21	0.92	0.21	0.12
$s_3\text{-}ts_0$	0.21	0.92	0.21	0.12
$s_4\text{-}ts_0$	0.21	0.92	0.21	0.12
$s_5\text{-}ts_0$	0.21	0.92	0.21	0.12
$s_6\text{-}ts_0$	0.21	0.92	0.21	0.12
				$\Sigma(s_i ts_k)$= 4.21

Estimates of overall transmitted S-R information for each task stimulus are given in Table S7 (also see Figure 2), and were computed as summed information across two levels in the putative hierarchy of sensorimotor information processing (i.e., s_1 in switch task= 2.61 + 3.61= 6.22 bits; s_1 in go/no-go task= 2.61 + 0= 2.61 bits, and in oddball task= 0.78 + 0= 0.78 bits).

Table S7. Summary of numerical values of transmitted information plotted in Figure 2.

	s_1	s_2	s_3	s_4	s_5	s_6
Switch	6.22	2.73	1.38	1.38	1.38	1.38
Go/NoGo	2.61	2.61	1.26	1.26	1.26	1.26
Oddball	0.78	0.78	0.78	0.78	1.26	1.26

References

Attneave, F. (1959). *Applications of information theory to psychology: A summary of basic concepts, methods and results*. New York: Holt, Rinehart and Winston.

Barceló, F., Periáñez, J. A., & Nyhus, E. (2008). An information theoretical approach to task-switching: evidence from cognitive brain potentials in humans. *Front Hum Neurosci, 1*, 13. doi: 10.3389/neuro.09.013.2007

Koechlin, E., & Summerfield, C. (2007). An information theoretical approach to prefrontal executive function. *Trends in Cognitive Sciences*, **11**, 229-235.

Miller, G.A. (1956). The magical number seven plus or minus two: some limits on our capacity for processing information. *Psychological Review*, 63, 81-97.